

Observation of a knee in the p+He energy spectrum below 1 PeV by using an hybrid measurement with ARGO-YBJ and a LHAASO Cherenkov Telescope

S.S. Zhang^{1*} and Z. Cao¹ for the LHAASO and ARGO-YBJ Collaboration[†]

¹ Key Laboratory of Particle Astrophysics, Institute of High Energy Physics, Chinese Academy of Sciences, 100049 Beijing, China.

E-mail: zhangss@ihep.ac.cn

The measurement of the cosmic ray energy spectrum, in particular for individual nuclei, is an important tool to investigate acceleration and propagation mechanisms. The determination of the "knees" in the spectra of different species is one of the main open problems in the cosmic ray physics. In fact, experimental results are still conflicting. In this paper we report a measurement of the mixed proton and Helium energy spectrum using the combination of the ARGO-YBJ experiment and of a wide field of view Cherenkov telescope, prototype of the future LHAASO experiment. The detectors are located at the Yangbajing Cosmic Ray Observatory (Tibet, P.R. China, 4300 m above sea level, 606 g/cm²). By means of a multi-parameter technique we selected a high purity proton plus Helium sample. A uniform energy resolution of about 25% throughout the whole investigated energy range (100 TeV - 3 PeV) is obtained. A knee-like feature at 700 ± 230 (*stat.*) ± 70 (*sys.*) TeV, with a clear steepening of the light component spectrum, is observed. This is in agreement with other two independent analysis of ARGO-YBJ data, and provides new important inputs to acceleration/propagation models for galactic cosmic rays.

*The 34th International Cosmic Ray Conference,
30 July- 6 August, 2015
The Hague, The Netherlands*

*Speaker.

[†]This work is supported in China by the Chinese Academy of Sciences (0529110S13), the Key Laboratory of Particle Astrophysics, Institute of High Energy Physics, CAS and in Italy by the Istituto Nazionale di Fisica Nucleare (INFN). The Knowledge Innovation Fund (H85451D0U2) of IHEP, China, the project 11475190, 10975145 and 11075170 of NSFC also provide support to this study. We acknowledge the essential support of W.Y. Chen, G. Yang, X.F. Yuan, C.Y. Zhao, R.Assiro, B.Biondo, S.Bricola, F.Budano, A.Corvaglia, B.D'Aquino, R.Esposito, A.Innocente, A.Mangano, E.Pastori, C.Pinto, E.Reali, F.Taurino and A.Zerbini.

Galactic cosmic rays are believed to originate at astrophysical sources, such as supernova remnants. The mechanism for accelerating nuclei to energies from 10^{14} eV to 10^{20} eV remains unknown. A handful of significant structures in the cosmic ray spectrum has been observed, the most important being the so-called “knee”, a clear steepening around 3×10^{15} eV [1, 2]. Many acceleration models have successfully explained the power-law characteristics of the spectrum, although no originating source has yet been experimentally observed for the high energy particles [3]. The knee of the spectrum obviously plays a key role to test the proposed acceleration and propagation models. One of the theories is that the knee marks the highest energy that the galactic cosmic ray sources can reach [4, 5]. The spectrum of all cosmic rays, however, does not appear to bend sharply, because different species may have different cut-off energies and extra-galactic cosmic rays may merge into the flux. These latter may dominate the flux at higher energies [6]. Such a straightforward investigation unfortunately has been very difficult in the past decades due to two experimental limitations. 1) direct measurements of cosmic ray spectra for specific nuclear species performed by space or balloon-borne detectors are constrained by their small exposures due to limited payloads, so that statistically reliable measurements cannot effectively extend to an energy higher than 10^{14} eV [7, 8], which is far below the knee; 2) Ground-based experiments with extensive air shower (EAS) techniques are troubled by large uncertainties such as large uncertainties on the energy scale and lack of effective tools to tag the nature of the primary inducing the observed showers, independently of the statistical accuracy of the measurement [9, 10]. As a consequence, the knee energy is found between 1 PeV and 6 PeV by different experiments as summarized in reference [1] mainly because of the unknown mixture and imprecise energy calibrations. The uncertainty in the attempts of measuring the pure proton spectrum is still large, e.g. the knee is found a few hundreds of TeV in CASA-MIA [11] and a few PeV in KASCADE [10]. The lack of well-measured knee energies for individual species is prohibitive for developing a precise theory about the origin of cosmic rays.

The situation is improved by the ARGO-YBJ experiment, at 4300 *m* above sea level in Tibet, which records nearly every secondary charged particle of showers incident upon its unique detector made of a continuous array of Resistive Plate Chambers (RPC) [12]. Such a set-up brings the threshold of the shower measurement by ARGO-YBJ down to the same energy range of CREAM [7]. This enables ARGO-YBJ to establish the energy scale by measuring the moon shadow [13] and cross-checking with CREAM [14, 15]. This improvement is enhanced with the addition of data from a Cherenkov telescope [16] imaging every shower in its field-of-view (FOV). The hybrid of the two techniques improves the resolution for shower energy measurements, and enhances the capability to discriminate showers induced by Hydrogen and Helium nuclei (*H&He*) from events initiated by heavier nuclei [17]. Here, we report the measurement of the knee of the energy spectrum of the light component (*H&He*) below 1 PeV using the hybrid data from the ARGO-YBJ RPC array and the Cherenkov telescope, which is a prototype of one of the main instruments in the future LHAASO experiment [18, 19].

1. The Hybrid Experiment

The hybrid experimental data set includes air showers whose core falls inside an area of $76m \times 72m$ fully covered by the ARGO-YBJ RPC array, i.e., 1 *m* from the edges of the array, and whose arrival directions are in the effective FoV of the telescope, i.e., a cone of 6° with respect to the

main axis of the telescope, which has a full FoV of $14^\circ \times 16^\circ$ pointing to 30° from the zenith. The telescope is about 79 m off the center of the array in the south-east direction. This defines a geometrical aperture of $163 \text{ m}^2 \text{ sr}$. According to the simulation of the hybrid experiment, high energy ($\geq 100 \text{ TeV}$) showers are detected with almost full efficiency, particularly the *H&He* events. This minimizes the uncertainty of the cosmic ray flux measurement.

In its FoV, the telescope [16] has an array of 256 pixels with a pixel size of approximately $1^\circ \times 1^\circ$. The shower image, which typically consists of more than ten pixels, records the accumulated Cherenkov photons produced in the entire shower development. By knowing the exact distance from the core, which is well measured by the RPC array, the total number of photons in the image can be used to reconstruct the shower energy. The image shape described by the Hillas parameters indicates the depth of the shower development after reaching its maximum, giving useful information to select proton or Helium showers. The ARGO-YBJ array consists of 1836 RPCs, each equipped with two analog readout “Big Pads” ($140\text{cm} \times 123\text{cm}$) to collect the total charge induced by particles passing through the chamber [20, 21]. The collected charge is calibrated to be proportional to the number of charged particles [21, 22, 23]. The most hit RPC, indicating the shower core, together with the surrounding RPCs, measures the lateral distribution of secondary particles within 5 m from the core. Such a unique measurement is very useful not only for a precise reconstruction of the shower geometry, but also for the selection of proton and Helium showers.

The coincident cosmic ray data, collected in the hybrid experiment from December 2010 to February 2012, are used for the analysis presented in this paper. The main constraint on the exposure of the hybrid experiment is the weather condition in the moon-less nights. The weather is monitored by using the bright stars in the FoV of the telescope and an infrared camera covering the whole sky. More details about the criteria for a good weather can be find elsewhere [17]. Combining the good weather conditions and the live time of the RPC array, the total exposure time is 7.28×10^5 seconds for the hybrid measurement. Further criteria (quality cuts) for well reconstructed showers in the aperture of the hybrid experiment are 1) at least 1000 particles recorded by the ARGO-YBJ digital readout [12] to guarantee high quality geometrical reconstruction of the shower fronts for required angular and core position resolution; 2) at least 6 pixels triggered in each shower image which is fully contained in the telescope FoV. About 32,700 events survived these cuts. The core and angular resolutions are better than 2 m and 0.3° , respectively.

A big number of extensive air showers, including their Cherenkov photons, are simulated by using the CORSIKA code [24] with the high energy hadronic interaction model QGSJETII-03 and with the low energy model GHEISHA. The G4argo [25] package and a ray-tracing procedure on the Cherenkov photons [26] are applied for further simulation of the detector responses. All five mass groups, i.e. proton, Helium, CNO (Carbon, Nitrogen and Oxygen) group, MgAlSi (Magnesium, Aluminum and Silicon) group and Iron are generated in the simulation. A detailed comparison between the data and the simulation can be found elsewhere [17].

2. Shower Energy Reconstruction and All-Particle Distribution

The shower energy, E , is reconstructed from the total number of photoelectrons, N_{pe} , in the shower image recorded by the telescope. This observable uses the whole atmosphere as a calorimeter to measure the energy deposited during the shower development. The number of photoelectrons

exponentially drops with the impact parameter R_p and therefore this effect has to be taken into account in the shower energy determination. Because of being shielded by the walls of the container, the effective area of the mirror varies with the space angle between the incident direction of the showers and the telescope main axis, denoted as α . Therefore, in the FOV of $14^\circ \times 16^\circ$ of the telescope, the N_{pe} still varies slightly with α . Using a very large sample generated by the simulation described above, a look-up table for the shower energy with three entries, i.e., N_{pe} , R_p and α , is determined for each mass group. For a shower with N_{pe} measured by the telescope and R_p and α measured by the RPC array, the shower energy can be read out from this table. The energy resolution is found symmetric and fits well a Gaussian function with σ between 23% and 27% for different mass group. However, a clear feature of the energy reconstruction is a systematic shift which depends on the nature of the primary. The difference between proton and Iron showers is approximately 37% as shown in the left plot of FIG. 1, significantly greater than the resolution. For a mixed sample with unknown composition, this feature will distort the all-particle energy spectrum even if the measurement is fully efficient.

In order to compare with other experiments or existing cosmic ray flux models without assuming any specific mixture of the species for the measured showers, in the right figure of FIG. 1 we plot the event distribution as a function of the measured N_{pe} . Also plotted in the same figure are the distributions generated according to the all-particle spectra measured by the experiments and the corresponding assumptions on the mixture of different species. Here we show the results from Tibet AS $_{\gamma}$ with two different composition models[27], from KASCADE with its composition models obtained from the unfolding procedures[10], and two widely quoted composition models, i.e., Hörandel [28] and H4a [29]. The comparison shows that the existing all-particle spectra and their corresponding composition models are in a general agreement at a level of 30%. The data used in this work also maintains a general agreement with others at a similar level.

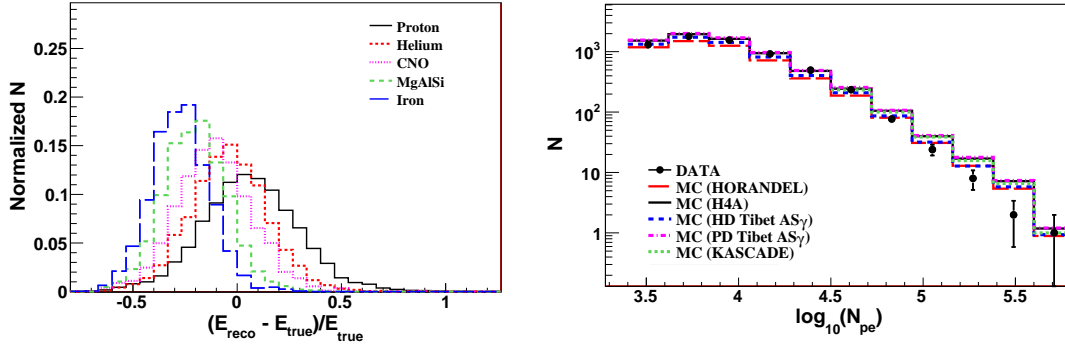


Figure 1: The simulated distribution of $(E_{true} - E_{reco})/E_{true}$ for different mass groups in the energy range 500 - 800 TeV is in the left figure. The reconstructed energy is obtained from the look-up table built for primaries p+He in 1 : 1 ratio. Distribution of the number of Cherenkov photo-electrons (N_{pe}) measured by the telescope (filled circles) is in the right figure. The histograms represent the N_{pe} distributions obtained by simulations according to the flux models [29, 28] and to the all-particle spectra and corresponding composition models reported by the Tibet AS $_{\gamma}$ [27] and KASCADE[10] experiments. The bin size is 0.22 in $\log_{10}N_{pe}$.

3. Hydrogen and Helium Event Selection

The secondary particles in showers induced by heavy nuclei are spread further away from the core region. Therefore significant differences of the lateral distributions exist in the vicinity of the cores between showers induced by light or heavy nuclei [23]. Beyond a certain distance, e.g., 20 m from the core, the lateral distributions become similar because they are mainly due to multiple Coulomb scattering of the secondary particles and are well described by the Nishimura-Kamata-Greisen (NKG) function. With its full coverage, the ARGO-YBJ array is the only detector able to measure the lateral distribution of the secondary particle density at the shower core. The number of particles recorded by the most hit RPC in an event, denoted as N_{max} , is a good parameter to discriminate between showers with different lateral distribution within 3 m from the cores. In a shower induced by a heavy nucleus, N_{max} is expected to be smaller than that in a shower induced by a light nucleus with the same energy [23]. Obviously, for a give primary mass, N_{max} also depends on the energy. We found from simulations that N_{max} is proportional to $(N_0^{pe})^{1.44}$ where N_0^{pe} is the total number of photo-electrons normalized to $R_p = 0$ and $\alpha=0^\circ$. We define a reduced dimensionless variable $p_L = \log_{10}N_{max} - 1.44\log_{10}N_0^{pe}$ to describe the N_{max} and N_0^{pe} correlation.

The shape of the shower image recorded by the Cherenkov telescope is also a mass-sensitive parameter. The elliptical image is described by the Hillas parameters [30], such as width and length. The images are more stretched, i.e., narrower and longer, for showers that are more deeply developed in the atmosphere. The length to width ratio (L/W) is therefore a parameter sensitive to the depth of the shower maximum which depends on the nature of the primary with the same impact parameter and the same energy. It is also known that the images are more elongated for showers farther away from the telescope, because of purely geometric reasons. The ratio L/W is nearly proportional to the shower impact parameter R_p , but depends very moderately on the shower size. Taking into account the dependence on measured number of Cherenkov photons in a shower and on the impact parameter, we define a reduced dimensionless variable $p_C = L/W - R_p/109.9m - 0.1\log_{10}N_0^{pe}$, obtained from the MC simulation, to absorb both the R_p and shower size effects.

The selection of the $H\&He$ sample is carried out by combining the two composition-sensitive parameters. A contour plot of the map for two mass groups, $H\&He$ and all other nuclei (C-N-O, Mg-Al-Si and Iron), is shown in FIG. 2. The cuts $p_L \geq -4.53$ or $p_C \geq 0.78$ result in a selected sample of $H\&He$ showers with a purity of 93% below 700 TeV and an efficiency of 72% assuming the composition models given in [28]. The aperture, given by the geometrical aperture of 163 $m^2 sr$ times the detection efficiency, gradually increases to 120 $m^2 sr$ at 300 TeV and keeps constant at higher energies. The contamination from the heavy nuclei increases with primary energy and depends on the composition. Assuming the Hörandel composition [28], the contamination of heavy species is found to be 13% at energies around 1 PeV, and gradually increases to 27% around 3 PeV. The associated uncertainty on the light component flux is discussed below.

The shower energy is now better defined because the intrinsic scale difference between H and He showers is smaller than 10%, significantly lower than the energy resolution. Using about 40,000 simulated events that survived all the reconstruction quality cuts and $H\&He$ selection, the energy resolution is found to be nearly constant, about 25%, and nearly offset-free, less than 3% throughout the entire energy range up to 3 PeV. This is important to identify any structure, such as bumps, dips or bends, in the spectrum.

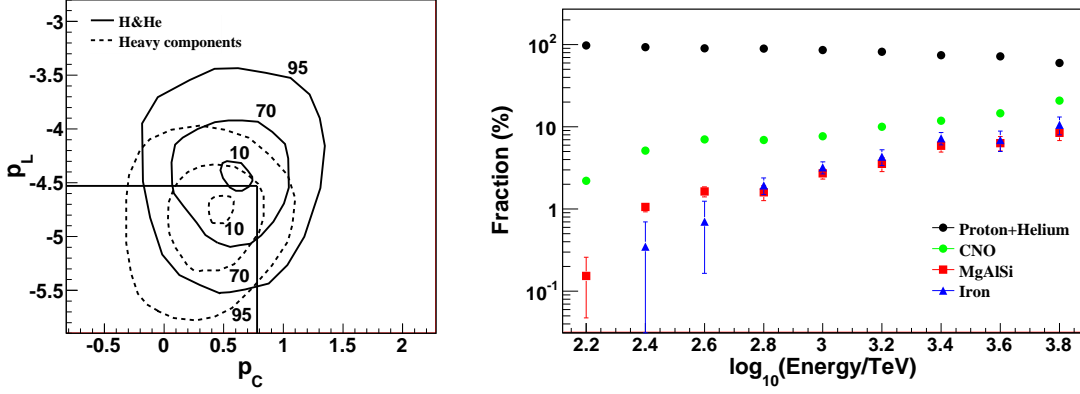


Figure 2: Composition-sensitive parameters p_L and p_C for the two mass groups, $H&He$ (solid contours) and heavier components (dashed contours) are in the left figure. The numbers on the contour isolines indicate the percentage of contained events. The fraction of events of different composition groups that survive the $H&He$ selection criteria is in the right figure. The heavy nuclei data indicates that the contamination increases with shower energy. The Hörandel model is assumed.

4. Energy Spectrum of Proton and Helium

Applying the criteria mentioned in Sect. 3 on the data set taken by the WFCT-02 and ARGO-YBJ hybrid experiment, the energy spectrum of the selected sample of $H&He$ showers is plotted in FIG. 3. To take into account the energy resolution and any kind of smearing like bin-to-bin migration from the true to the reconstructed primary energy, a Bayesian algorithm [31] is applied to unfold the observational data.

A stricter cut for higher purity (97%) $H&He$ sample has been applied below 700 TeV [17] where the spectrum fits well with a single-index power law, according to CREAM[7] and ARGO-YBJ[14, 15]. This corresponds to a much smaller aperture of $\sim 50 m^2 sr$ with a $H&He$ selection efficiency of 30%, with a negligible contamination from heavy nuclei and a corresponding precise measurement of the spectrum [17] shown by the filled squares in FIG. 3. This allows a check of both energy scale and absolute flux once compared with the previous measurements. The difference between the fluxes measured by the above experiments is found less than 9%[17].

An evident bending structure is observed in the cosmic $H&He$ spectrum by the hybrid experiment at 4300 m above sea level. The measured spectrum can be fitted by a broken power law, with a broken energy $E_k = 700 \pm 230$ TeV and $\chi^2/dof = 0.5$. The index below the break is -2.56 ± 0.05 and the index above the break is -3.24 ± 0.36 . The relatively large error on E_k is due to the limited statistics and the energy resolution. In addition, the systematic error in the energy scale is 9.7%, which corresponds to ~ 70 TeV at E_k [17].

Systematic uncertainties on the measured flux mainly arise from the following causes: 1) The contamination of heavy nuclei cannot be unambiguously determined since it depends on the elemental composition of cosmic rays, that is unknown in the energy range considered here. The contamination increases with energy, from about 2.5% of the measured $H&He$ flux at 158 TeV to about 13% at 1 PeV evaluated by the Hörandel composition [28]. Obviously, if the heavy compo-

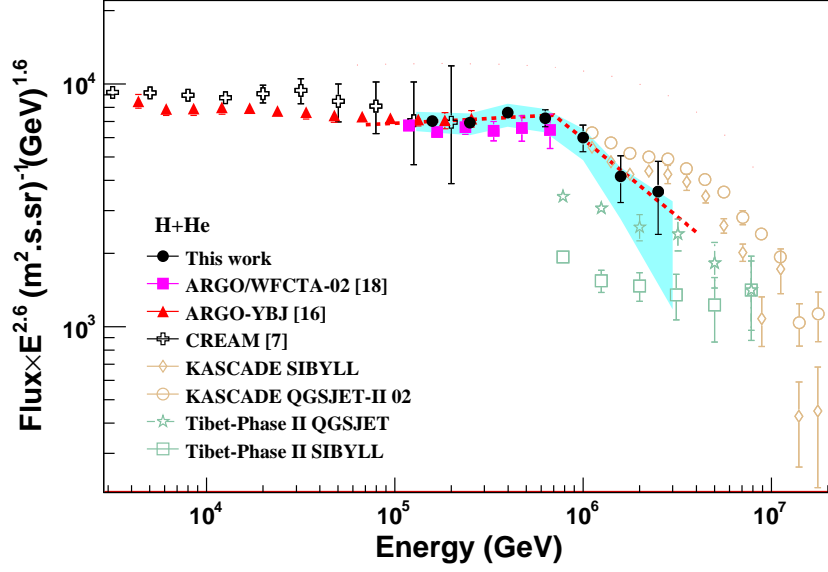


Figure 3: $H&He$ spectrum by the hybrid experiment with ARGO-YBJ and the imaging Cherenkov telescope. A clear knee structure is observed. The $H&He$ spectra by CREAM [7], ARGO-YBJ [15] and the hybrid experiment [17] below the knee, the spectra by Tibet AS γ [9] and KASCADE[10] above the knee are shown for comparison. The shaded areas represent the systematic uncertainty.

nents would be more abundant than what described by the existing model, the contamination could be proportionally larger. 2) due to a slightly different detection efficiencies for $H&He$ showers, the fraction of Helium in the selected samples depends on the composition assumption. This also results in an uncertainty of 3% in the overall flux. 3) Choice of the interaction models. The overall flux uncertainty is about 4.2% by considering the high energy interaction models SIBYLL and QGSJET, and the low energy interaction models GHEISHA and FLUKA. 4) Boundary effect of the aperture. Due to the core resolution and angular resolution, the corresponding flux uncertainty is about 3% by comparing the selection boundary and the real geometrical boundary. 5) The flux uncertainty of 7% is found by considering the uncertainties on the calibration of the number of particles measured by the RPCs described in ref. [22]. The overall systematic uncertainty on the flux is plotted as the shaded area in FIG. 3.

5. Discussion and conclusions

In summary, the joint operation of the ARGO-YBJ detector with a wide field-of-view and imaging Cherenkov telescope allowed a detailed investigation of the energy range bridging the gap between the direct observations of CREAM and the ground-based KASCADE experiment. The data of the hybrid experiment show a clear steepening of the flux of these light elements starting at an energy of about 700 TeV. The knee below 1 PeV is also consistent with two independent analyses of ARGO-YBJ data by using the RPC charge readout only [32, 33]. The observation of the knee of the primary light component at such a low energy gives fundamental inputs to galactic cosmic ray acceleration models.

References

- [1] J. Blümer et al. Progress in Particle and Nuclear Physics 63, 293 (2009)
- [2] G. Kulikov, G. Khristiansen, JETP 35, 635 (1958)
- [3] J.R. Hörandel, Astropart. Phys. 21, 241 (2004)
- [4] A D Erlykin and A W Wolfendale, J. Phys. G: Nucl. Part. Phys. 23, 979 (1997)
- [5] E.G. Berezhko H.J.Völk, The Astrophys. J., 661, L175 (2007)
- [6] V.Berezinsky, A.Z.Gazizov, S.I.Grigorieva, Phys. Rev. D 74, 043005 (2006)
- [7] Y. S. Yoon et al., Astrophys. J. 728, 122 (2011)
- [8] A. Panov et al., arXiv:astro-ph/0612377
- [9] M. Amenomori et al., Advances in Space Research 47, 629 (2011)
- [10] T. Antoni et al., Astrop. Physics 24, 1 (2005); W.D. Apel et al. Astrop. Physics 31, 86 (2009); W.D. Apel et al., Astrop. Physics 47, 54 (2013)
- [11] M.A.K. Glasmacher *et al*, Astrop. Physics 12, 1 (1999)
- [12] G.Aielli et al. Nucl. Instr. and Meth. A 562, 92 (2006)
- [13] B. Bartoli et al., Phys. Rev. D84, 022003 (2011)
- [14] B. Bartoli et al., Phys. Rev. D 85, 092005 (2012)
- [15] B. Bartoli et al., arXiv:1503.07136 [hep-ex] (in press on Phys. Rev. D), (2015)
- [16] S.S. Zhang et al., Nucl. Instr. and Meth. A 629, 57 (2011)
- [17] B. Bartoli et al., Chinese Physics C, Vol. 38, 045001 (2014)
- [18] Z. Cao et al., Chinese Physics C 34, 249 (2010)
- [19] H.H. He et al., LHAASO Project: detector design and prototype, 31st ICRC, LODZ, (2009)
- [20] M. Iacovacci et al., Nucl. Phys. B 136, 376 (2004)
- [21] B. Bartoli et al., Astrop. Physics 67, 47 (2015)
- [22] B. Bartoli et al., Nucl. Instr. and Meth. A 783, 68 (2015)
- [23] I. De Mitri, On behalf of the ARGO-YBJ Collaboration, Nucl. Instr. and Meth. A 742, 2 (2014)
- [24] D. Heck et al., 1998 Thouw, Report No. FZKA 6019, Forschungszentrum
- [25] Guo Yi-Qing et al., Chinese Physics C 34, 555-559 (2010)
- [26] J L Liu et al., J. Phys. G: Nucl. Part. Phys. 36, 075201 (2009)
- [27] M. Amenomori et al., Phys. Rev. D, Volume 62, 112002 (2000) and Astrophys. J. 678, 1165 (2008)
- [28] J.R. Hörandel, Astrop. Physics 19, 193 (2003)
- [29] T.K. Gaisser *et al*, Astrop. Physics 35, 801 (2012)
- [30] A. M. Hillas. 19th ICRC, volume 3, page 445, La Jolla, 1985
- [31] G. D' Agostini, Nucl. Instrum. Methods Phys. Res., Sect. A 362, 487 (1995)
- [32] P. Montini et al., (ARGO-YBJ coll.), in Proc. 34th ICRC, (The Hague, 2015) ID: 961
- [33] A. D' Amone et al., (ARGO-YBJ coll.), in Proc. 34th ICRC, (The Hague, 2015) ID: 917